Self-Assembly of Styrylthiophene Amphiphiles in Aqueous Dispersions and Interfacial Films: Aggregate Structure, Assembly Properties, Photochemistry, and Photophysics

Xuedong Song, Jerry Perlstein, and David G. Whitten*

Department of Chemistry and NSF Center for Photoinduced Charge Transfer, University of Rochester, Rochester, New York 14627, and Chemical Science and Technology Division, Los Alamos National Laboratory, Los Alamos, New Mexico 87545

Received: October 22, 1997; In Final Form: December 2, 1997

Fatty acids and phosphatidyl choline derivatives incorporating the photoreactive *trans*-styrylthiophene chromophore have been prepared and studied in Langmuir−Blodgett films and aqueous dispersions, respectively. Both absorption and fluorescence spectra in the assemblies show prominent shifts indicative of aggregation similar to that observed with similar *trans*-stilbene and *trans*-azobenzene derivatives previously investigated. Studies of aqueous dispersions of the pure styrylthiophene phospholipids indicate the formation of structures much larger than the typical small unilamellar bilayer vesicles formed from saturated phospholipids of comparable chain length. Studies of the disaggregation process for two of the phospholipids give aggregation numbers of approximately 2 and 6, corresponding to 4 and 12 styrylthiophene units per aggregate. The stability of these aggregates is very similar to those of corresponding stilbene aggregates, and on the basis of spectral similarities it seems reasonable to propose a "pinwheel" fraction of a glide or herringbone structure as the "unit aggregate" and predominate species present in the aqueous dispersions. However, the chief photoreaction observed for the aqueous dispersions of the phospholipids is dimerization to form the syn head-to-head dimer, consistent with topologically controlled reaction from a translation structure in which nearest-neighbor chromophores are aligned parallel. Simulations suggest that while a translation layer structure may be of lowest energy, glide layer structures that show good agreement between measured and predicted properties are also energetically accessible. A possible explanation for the observed reactivity and photophysics is that within the aqueous dispersions there may be equilibration between "glide" and "translation" structures. When mixtures of the styrylthiophene phospholipids and saturated phospholipids are codispersed, bilayer vesicles are formed that are capable of entrapping reagents such as carboxyfluorescein. Irradiation of the aggregated *trans*-styrylthiophene in these vesicles leads to release of the entrapped carboxyfluorescein concurrent with photodimerization of the styrylthiophene. The pattern of reagent release is similar to that observed upon photoisomerization of the corresponding azobenzene aggregates and suggests a "catastrophic" destruction of the vesicles.

Introduction

A number of recent investigations have shown that the "normal" tendency of amphiphiles to self-assemble to form micelles or bilayer dispersions in water or interfacial films such as Langmuir−Blodgett (LB) monolayers at the air−water interface can be modified or enhanced when aromatic groups or other substituents possessing extended π-conjugation are incorporated into the amphiphile structure.[1−8] Studies with fatty acids and phospholipids containing *trans*-stilbene,[2] *trans*-azobenzene,[3] or diphenylacetylene units[5] have shown enhanced tendencies for self-association that manifest themselves in terms of tight aggregation of the chromophores with pronounced shifts in absorption and emission spectra, higher phase transition temperatures for the phospholipid suspensions in water (as well as persistence in the spectral shifts associated with the aggregation above the phase transition temperature), resistance of the aggregated amphiphiles to dispersion upon dilution with saturated fatty acid or phospholipid hosts in both films and aqueous bilayers, and a tendency for several of the modified phospholipids to form much larger macroscopic structures than the small unilamellar vesicles generally obtained on dispersion of saturated phospholipids and other double-chain surfactants having saturated alkyl chains.[2,3] In several cases[2−4] both experimental studies and simulations support a structure for the aggregated chromophores in which both small unit aggregates (small limiting clusters) and extended structures have a glide or herringbone arrangement of the chromophores characterized by favorable noncovalent interactions that appear to be predominantly edge-to-face,[9] similar to that found in both experimental and theoretical studies of the benzene dimer.[10] A unit aggregate in the case of a "pinwheel" tetramer and its extended mosaic glide layer are shown schematically in Figure 1. The strong excitonic interactions observed in the absorption spectra of the aggregated aromatics or dyes are well-modeled in calculations using the extended dipole−extended dipole treatment of Kuhn and co-workers.[11] That these noncovalent interactions can be a strong force in controlling self-assembly is also indicated by the finding that films at the air−water interface often show the aggregate as the predominant species, even before compression results in close packing of the amphiphiles.[7] While these interactions manifest themselves most strongly in aqueous dispersions and at the air−water interface, they can also be observed as an influencing factor in other contexts in different media. For example, dyads linking a cholesterol moiety with

S1089-5639(97)03421-X CCC: $15.00
Published on Web 02/14/1998

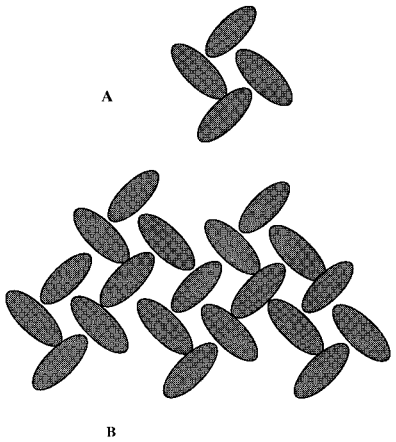

Figure 1. Schematic representation of (A) "pinwheel" tetramer of aromatic amphiphile (as seen from above) showing edge−face interactions between neighboring π-systems and (B) a mosaic of these fragments into a growing "glide" or herringbone array.

trans-stilbene,[12] *trans*-azobenzene,[13] or squaraine dyes[14] exhibit "supergelating" abilities in a variety of organic solvents; formation of the gel is accompanied by spectral shifts from monomer in solution, in some cases, to spectra similar to those observed in the aqueous dispersions and interfacial films. Similar molecules containing cholesterol, but no aromatic chromophore, do not show comparable gelating tendencies. When the monomer aromatic is photoreactive (e.g., *trans*-stilbene), photoreactivity is often modified or eliminated in aggregate assemblies. However, for the assemblies of the azobenzene-derivatized amphiphiles[3] and gelators[13] irradiation does result in *trans*−*cis* isomerization, although with reduced efficiencies, and in many cases with strong disruption of the structured assemblies. We have found, for example, that mixed vesicles containing azobenzene-derivatized phospholipids undergo release of entrapped reagents upon photolysis, concurrent with photoisomerization.[13] The large structures formed by extended arrays of azobenzene phospholipids are completely destroyed as photoisomerization occurs, and indications are that the *cis*-azobenzene phospholipids must form much smaller and less organized structures.

While the glide or herringbone structure is often found both experimentally and in simulations to be the likely structure for these aggregates,[2−4,15] simulations frequently suggest that translation layer structures may be close in energy. Since these are gas-phase simulations, which do not permit the estimation of solvent−solute interactions, any one of several low-energy minima from the gas-phase calculations may be considered to be of comparable probability for the structure in the actual systems studied in which solvent−solute interactions play a critical role. For example, the styrene amphiphiles **1** and **2** (Chart 1) form LB films and vesicles, respectively, in which there are small spectral shifts compared to the above-described systems and the present work.[16] The aggregation and consequent reactivity seem most consistent with a translation-layer structure in which there are noncovalent interactions that are predominantly face-to-face or "π-stacking". Both of these assemblies yield a single cyclobutane photodimer upon irradiation, which has been shown to be the β or syn head-to-head product. Simulations clearly predict that the lowest energy configurations should be translation layers and the structure that most closely predicts experimentally measurable properties such as the exciton splitting, "tilt angle" of the chomophore and area/molecule in the condensed film is a translation layer array in which the two double bonds of nearest-neighbors are aligned and separated by 4.10 Å, which is within the "magic distance" of 3.5−4.2 Å for photodimerization of several olefins such as cinnamic acid derivatives in the crystalline state.[17]

CHART 1

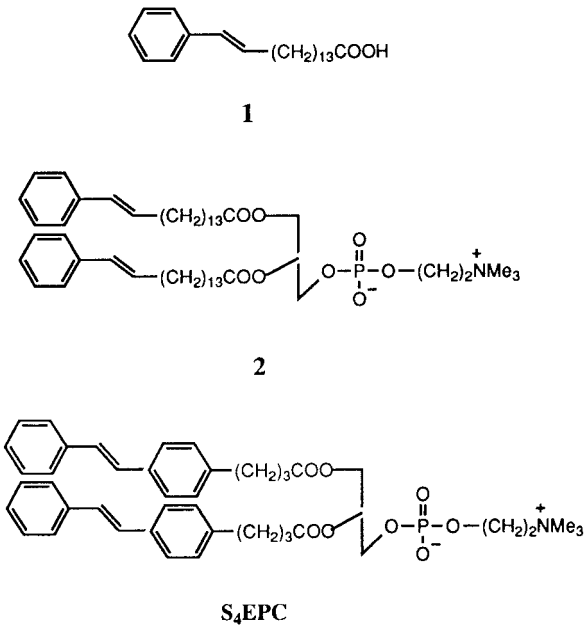

1

2

S_4EPC

The styrylthiophene chromophore is formally similar to stilbene and might be expected to exhibit similar photophysical and photochemical behavior. *trans*-Styrylthiophene shows a similar intense absorption spectrum in the ultraviolet, with the long wavelength band red-shifted compared to *trans*-stilbene but with a B band at nearly the same energy. Irradiation of *trans*-styrylthiophene has been reported to result in isomerization but to little dimerization.[18] In the crystal *trans*-styrylthiophene is photostable, as predicted from the crystal structure that shows unfavorable packing for topologically controlled dimerization.[19] Substituted *trans*-styrylthiophene derivatives have been found to exhibit both photoisomerization and photodimerization in solution as well as photodimerization in the solid state in some cases.[19a] In the present paper we report the synthesis and investigation of fatty acid and phospholipid derivatives incorporating the styrylthiophene chromophore at the end of a hydrocarbon chain. We find that these amphiphiles exhibit similar behavior to the above-mentioned aromatic derivatized amphipihles in terms of exhibiting aggregate formation, concurrent with pronounced changes in absorption spectra and photophysical behavior. Although many aspects of the observed behavior suggest the predominance of aggregates quite similar to those observed for stilbene, azobenzene, and squaraine derivatives,[2−4] we find the chief photoreaction that occurs for suspensions of the phospholipids in water is photodimerization to give a major product that appears to derive from a topological control in the bilayer similar to that observed for styrene **2**.[16] We find that mixtures of the styrylthiophene with saturated phospholipids result in the formation of vesicles that can entrap reagents such as carboxyfluorescein. Interestingly, we find that irradiation of these vesicles under conditions producing photodimerization results in rapid and nearly complete release of the entrapped reagents.

Experimental Section

Materials and General Techniques. Synthetic reagents were purchased from Aldrich Chemical Co. and used as received

CHART 2

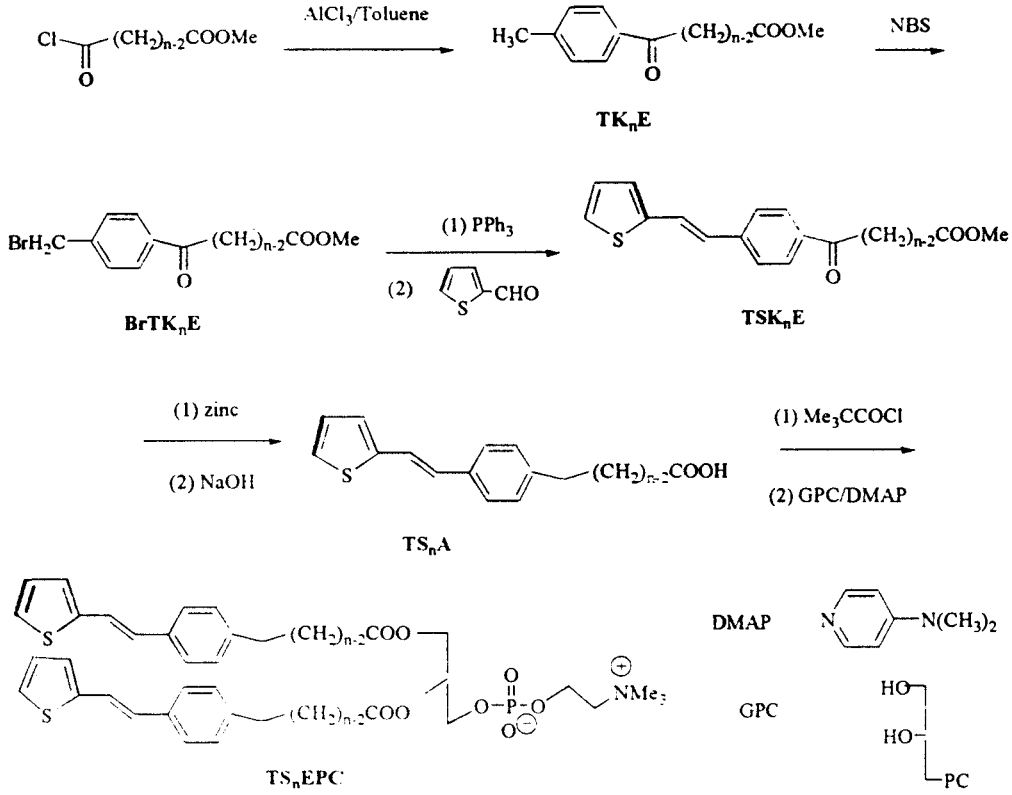

unless otherwise stated. α-, β-, and γ-cyclodextrins (CDNs, 99+%) were purchased from Aldrich. L-α-glycero-3-phosphorylcholine as the cadmium chloride complex, L-α-dimyristoyl phosphatidylcholine (DMPC, 99+%), and L-α-dipalmitoyl phosphatidylcholine (DPPC, 99%) were obtained from Sigma. All solvents for spectroscopic studies were spectroscopic grade from Fisher or Aldrich. Milli-Q water was obtained by passing in-house distilled water through a Millipore-RO/UF water purification system. Deuterated solvents were purchased from MSD Isotopes or Cambridge Isotope laboratories.

Melting points were taken on an El-Temp II melting point apparatus and are uncorrected. Proton NMR spectra were recorded on a General Electric QE300 MHz spectrometer using deuterated solvent locks. FAB mass spectra were measured at the Midwest Center for Mass Spectrometry. Absorption spectra were obtained on a Hewlett-Packard 8452A diode array spectrophotometer. The circular dichroism (CD) study was carried out on a JASCO J-710 spectropolarimeter. Fluorescence spectra were recorded on a SPEX Flurolog-2 spectrofluorimeter and were uncorrected. Differential scanning calorimetry (DSC) measurements were carried out on a MC-2 Ultrasensitive Scanning Calorimeter from MicroCal, Inc. Size extrusion experiments for the particles in aqueous dispersions of amphiphiles were performed with an extruder through CoStar Nucleopore Polycarbonate Filters. Dynamic light scattering measurements were carried out at the Eastman Kodak research laboratories. All samples were routinely filtered through a 1.2-μm nylon syringe filter before data acquisition. A 200-W Mercury lamp (Oriel) or a photochemical reactor (Rayonet, The Southern New England Ultraviolet Company) was used for irradiation. The 365-nm line was separated through an interference filter (365 BP 10, $T = 217$).

The general methods used for preparing Langmuir−Blodgett (LB) films and self-assemblies are based on techniques described by Kuhn and co-workers.[20] Monolayers of chromophore-derivatized fatty acids or phospholipids were prepared by spreading a chloroform solution of material to be studied onto an aqueous surface containing cadmium chloride (2.5×10^{-4} M) and sodium bicarbonate (3×10^{-5} M, pH = 6.6−6.8) on a KSV 5000 automatic film balance at room temperature (23 °C). The monolayers were then transferred onto quartz substrates. Quartz glass slides were cleaned sequentially in chloroform and detergent and followed by "piranha" solution (30% H_2O_2/H_2SO_4) cleaning for 30 min. The quartz substrates were rinsed throughly in Milli-Q water and dried before use in the LB assemblies. Reflectance spectra for the monolayers at the air/water interface were recorded with a SD1000 fiber optics spectrometer (Ocean Optics, Inc.) equipped with optical fibers, an LS-1 minature tungsten halogen lamp, and a CCD detector. Bilayer vesicles were prepared according to established protocols.[21] A Cell Disrupter W220F from Heat Systems Ultrasonics, Inc. (setting 6.5, 35w) was used for probe-sonication. Aggregate size measurements are similar to the procedures used for azobenzene-derivatized phospholipid (APLs)[3] and stilbene-derivatized phospholipids (SPLs).[2] The fluorescence lifetime measurements are described elsewhere.[5]

Identification of Photoproducts for Aggregates. An aqueous dispersion of TS_4EPC (11 mg, see Chart 2 for its structure) was irradiated in a photochemical reactor using ultraviolet light until the blue-shifted absorption band of the aggregates disappeared. Sodium hydroxide (5 equiv) was added to the reaction mixture followed by stirring at 45 °C for 24 h. The mixture was acidified by 5% hydrochloric acid to pH = 2, and the products were extracted with chloroform. Chloroform was removed, and the residue was dissolved in methanol containing a drop of concentrated sulfuric acid followed by refluxing for 2 h. The sulfuric acid was neutralized by sodium bicarbonate, and the solvent was removed. TLC (chloroform/methanol = 95/5) showed one major spot and one minor spot for the residue. No product was observed in the absence of irradiation. The

major photoproduct was separated by silica gel chromotagraphy to give an oil. ^{1}H NMR (500 MHz, CDCl3), δ: 6.8−7.3(m, 14H), 4.55(dd, 4H), 3.70(s, 6H), 2.55(t, 4H), 2.25(t, 4H), 1.90-(m, 4H). FAB: calcd for $[M + H]^+$, 573.2; found, 573.2

Synthesis of Styrylthiophene Derivatives. The synthesis of the styrylthiophene derivatives investigated in this study with their acronyms is outlined in Chart 2.

BrTK$_8$E: Methyl suberyl chloride (2.1 g) in 10 mL of toluene was added dropwise to a mixture of $AlCl_3$ (9 g) and dry toluene (40 mL) at 0 °C. The reaction mixture was allowed to warm to room temperature over 3 h and then decanted into ice water. Ether was used to extract the product, and the ether layer was then washed with 5% $NaHCO_3$ aqueous solution. After the ether was removed, a raw product (9.1 g) was obtained, which was pure enough for bromination.

The raw product (5.3 g) obtained above together with *N*-bromosuccinimide (NBS, 4.8 g) in CCl_4 (100 mL) was gently refluxed for 5 min, followed by irradiation with a sunlamp to initiate the reaction. The reaction was complete in 10 min, and the product, a precipitate, was separated by filtration. After the solvent was removed, the residue was recrystallized in THF/hexane to give white needle crystals (3.4 g, 49%). ^{1}H NMR (300 MHz, $CDCl_3$), δ: 7.95 (d, 2H), 7.51(d, 2H), 4.53(s, 2H), 3.70(s, 3H), 2.95(t, 2H), 2.35(t, 2H), 1.4−1.8(m, 10H).

TSK$_8$E: A mixture consisting of BrTK$_8$E (2.4 g) and triphenylphosphine (3.1 g) in dry xylene (100 mL) was refluxed for 4 h and then cooled to room temperature. The precipitate (3.2 g) that was produced was collected and dissolved in a solvent mixture consisting of methylene chloride (25 mL) and tetrahydrofuran (50 mL). To this solution was added potassium carbonate (3.6 g), 18-crown-6 (20 mg), and 2-thiophenecarboxaldehyde (2 mL). The mixture was refluxed for 12 h, and a dark solid was separated by filtration. The solvent was removed, and the residue was purified by a silica gel column using CH_2Cl_2/hexane = 1/1 as eluent to give TSK$_8$E (0.8 g, 32%). ^{1}H NMR (300 MHz, $CDCl_3$), δ: 7.97(d, 2H), 7.58(d, 2H), 7.39(d, 1H), 7.35−7.05(m, 2H), 7.09(t, 1H), 6.97(d, 1H), 3.69(s, 3H), 2.98(t, 2H), 2.35(t, 2H), 1.8−1.4(m, 10H).

TS$_8$A: Two grams of zinc dust was washed with 5 mL of 10% hydrochloric acid for 1 min followed by three washings of distilled water. To the zinc was added 5 mL of amalgamating solution (containing 5 mL of concentrated hydrochloric acid, 50 mL of water, and 5 g of mercuric chloride). The mixture was agitated for 1 min, followed by three washings of distilled water. To the amalgamated zinc was added 10 mL of 25% hydrochloric acid, 20 mL of toluene, and 800 mg of TSK$_8$E. The mixture was refluxed with fast stirring. TLC (hexane/acetone = 4/1 as eluent) showed complete disappearance of the starting material after 20 min. After the mixture cooled to room tempertaure, the toluene layer was collected and the solvent was removed. The residue was purified by a silica gel column using hexane/acetone = 4/1 as eluent to afford 300 mg of white crystals (41%). ^{1}H NMR (300 MHz, CD_3OD), δ: 7.4-(d, 2H), 7.29(d, 1H), 7.25(s, 1H), 7.16(d, 2H), 7.10(d, 1H), 7.02-(t, 1H), 6.92(d, 1H), 3.65(s, 3H), 2.62(t, 2H), 2.34(t, 2H), 1.61(m, 4H), 1.35(m, 6H).

A mixture containing the white crystals (300 mg) obtained above, potassium hydroxide (0.5 g), water (5 mL), and acetone (10 mL) was refluxed for 0.5 h, and the acetone was then removed. The aqueous phase was acidified using 10% hydrochloric acid, and the precipitate was collected. The raw product was recrystallized from a mixed solvent of acetone and water to give white crystals (250 mg, 87%); mp, 124−125 °C. ^{1}H NMR (300 MHz, CD_3OD), δ: 7.41(d, 2H), 7.29(d, 1H), 7.24-(s, 1H), 7.16(d, 2H), 7.10(d, 1H), 7.02(t, 1H), 2.66(t, 2H), 2.34-(t, 2H), 1.61(m, 4H), 1.30(m, 6H).

TS$_8$EPC: The synthesis is similar to the reported procedures.[5,22] Yield: 44%. ^{1}H NMR (300 MHz, $CDCl_3$), δ: 7.40-(d, 4H), 7.26−7.10(m, 8H), 7.08(d, 2H), 7.02(t, 2H), 6.90(d, 2H), 5.24(m, 1H), 4.40(m, 3H), 4.16(m, 1H), 4.00(m, 2H), 3.88-(m, 2H), 3.37(s, 9H), 2.60(t, 4H), 2.32(m, 4H), 1.60(m, 8H), 1.30(m, 12H). FAB: *m/z* calcd for $[M + H]^+$, 878.3; found, 878.3.

TS$_4$A: The preparation procedure is identical with that for TS$_8$A. Yield, 59%; mp, 126−128 °C. ^{1}H NMR (300 MHz, CD_3OD), δ: 7.48(d, 2H), 7.30(m, 2H),7.20(d, 2H), 7.17(m, 1H), 6.99(m, 1H), 6.93(d, 2H), 2.67(t, 2H), 2.33(t, 2H), 1.91(m, 2H).

TS$_4$EPC: The synthesis is similar to that for TS$_8$EPC. Yield: 67%. ^{1}H NMR (300 MHz, $CDCl_3$), δ: 7.38(d, 4H), 7.15−7.10(m, 8H), 7.07(d, 2H), 7.02(t, 2H), 6.90(d, 2H), 5.28-(m, 1H), 4.42(m, 3H), 4.20(m, 1H), 4.08(m, 2H), 3.90(m, 2H), 3.37(s, 9H), 2.66(m, 4H), 2.35(m, 4H), 1.95(t, 4H). FAB: calcd for $[M + H]^+$, 766.2; found, 766.2.

TABLE 1: Absorption and Fluorescence Data for TPLs and TS$_8$A in Different Media

compounds	media	λ_{max}^{abs} (ϵ_{max})[c]	λ_{max}^{em} (QY[a])	$\Delta\lambda^{abs}$ [b] (nm)	$\Delta\lambda^{em}$ [b] (nm)
TS$_8$EPC	$CHCl_3$	332(5.04)	388(0.041)		
	H_2O	290(3.74)	426(0.33)	42	40
	LB film	286	427	46	41
	DMPC	334(4.91)			
TS$_4$EPC	$CHCl_3$	332(5.39)	388(0.032)		
	H_2O	306(3.93)	426(0.13)	26	40
	DMPC	334(5.13)			
TS$_8$A	$CHCl_3$	332	388		
	LB film	286	427	46	41
	monolayer[d]	286		46	

[a] Quantum yield, stilbene in methyl cyclohexane as reference. [b] Spectral shifts relative to those for monomer. [c] Extinction coefficient ($\times 10^{-4}$). [d] Monolayer film at the air−water interface.

Results

Preliminary Characterization of Styrylthiphene Amphiphiles in Dilute Solution, Aqueous Dispersions, and Langmuir−Blodgett Films. The structures of the fatty acid and phospholipid derivatives used in this study are shown in Chart 2 together with their acronyms. Both the fatty acids and phospholipids are soluble in organic solvents such as chloroform or methylene chloride. For both sets of compounds dilute solutions show an intense absorption in chloroform (A band) at 332 nm and fluorescence with a maximum at 388 nm, which are indistinguishable from those of the alkyl-substituted *trans*-styrylthiophene monomer. Compared to that of *trans*-stilbene, these spectra are similar but with less structure and with red-shifts of 17 and 32 nm for absorption and fluorescence, respectively. Aqueous dispersions of the phospholipids TS$_4$-EPC and TS$_8$EPC, prepared by sonication, give clear solutions that scatter light and that exhibit blue-shifted absorption and red-shifted fluorescence spectra relative to those for the same compounds in chloroform. Dispersions of TS$_4$EPC and TS$_8$-EPC in water with an excess of saturated phospholipid such as dimyristoyl phosphatidyl choline (DMPC) give absorption spectra slightly broader than those obtained in chloroform, while the fluorescence appears nearly identical with that in organic solvents. Data for absorption and fluorescence spectra in different media are listed in Table 1. Figure 2 compares absorption and fluorescence spectra of TS$_4$EPC in different media.

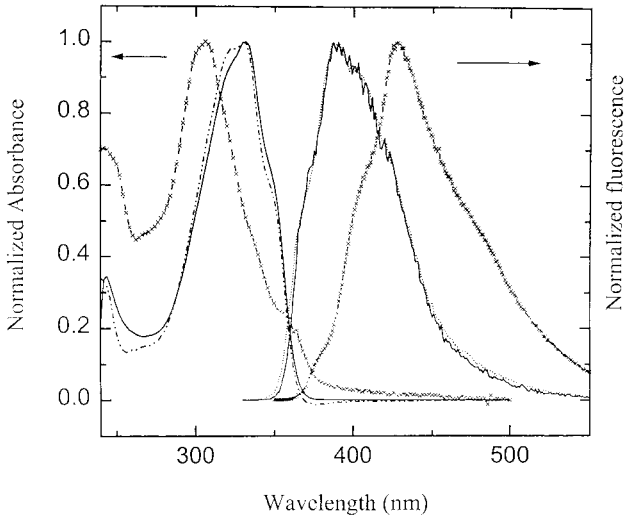

Figure 2. Absorption and fluorescence spectra of TS_4EPC in different media: — in chloroform, —×— in water, —••— in DMPC.

Both TS_8A and TS_8EPC form insoluble monolayer films upon dispersion from chloroform at the air−water interface. TS_4A, however, is too soluble in water to form an LB film. The films of TS_8A exhibit pressure−area isotherms similar to those of the *trans*-stilbene fatty acids and saturated fatty acids with a limiting area/molecule of 22−24 Å.[2] This suggests close packing into a highly ordered, near-crystalline array. The films are easily transferred to rigid supports such as quartz with qualitatively similar spectra to those for the aqueous dispersions of TS_8EPC. In contrast, films of TS_8EPC however exhibit a much broader isotherm, and the films are not easily transferred to quartz slides. For compression of the films of TS_8EPC, an early phase change is observed followed by a moderately steep rise to a limiting area of 30 $Å^2$/molecule; at this point it appears a bilayer may be forming since a limiting area/molecule for a two-chain amphiphile would be expected to be signficantly larger. Both films show the same blue-shifted absorption. As was previously observed for the stilbene[2] and azobenzene[3] amphiphiles, studies of the reflectance spectra of films of TS_8A and TS_8EPC at the air−water interface show essentially constant (blue-shifted) spectra before, during, and after compression suggesting that whatever interaction exists between chromophores in the amphiphiles does not occur as a consequence of the compression.

Both TS_4A and TS_8A are rendered more water soluble upon addition of α-, β-, or γ-cyclodextrins; the effect is particularly noticeable in the case of TS_8A. The complex of TS_8A with β-cyclodextrin shows similar absorption and fluorescence to the spectra obtained in chloroform; however, the spectra for TS_8A in the presence of α-cyclodextrin are noticeably sharper, and the fluorescence is much more intense (see below). In contrast, the complex of TS_8A with γ-cyclodextrin gives a slightly blue-shifted absorption, which is similar to those of the TS phospholipids in water with excess DMPC. The fluorescence of TS_8A in γ-cyclodextrin is broadened and red-shifted compared to the monomer in the other cyclodextrins and similar to that for the TS phospholipids in water. Figure 3 compares absorption and emission spectra of TS_8A in the presence of the different cyclodextrins. Figure 4 compares absorption and fluorescence spectra of TS_8A, TS_8EPC, and TS_4EPC in the several different environments discussed above. While TS_8A exists in cyclodextrin solutions almost exclusively as the complex, solutions of TS_4A in the presence of the different cyclodextrins show only a trace amount of complex formation.

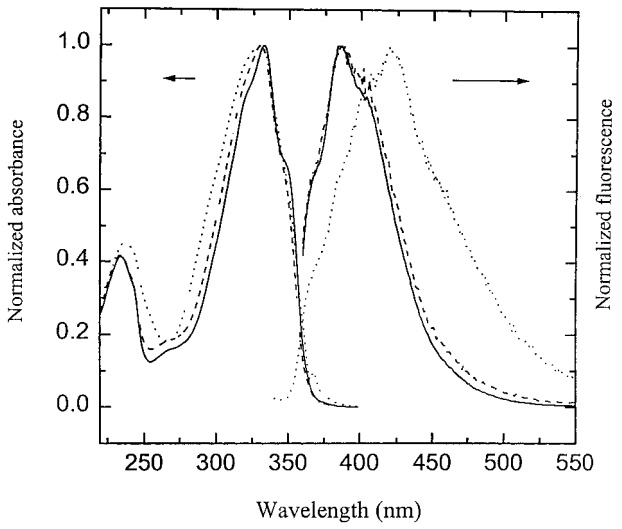

Figure 3. Normalized absorption and fluorescence spectra of TS_8A in cyclodextrins: — α-cyclodextrin, - - - β-cyclodextrin, ••• γ-cyclodextrin.

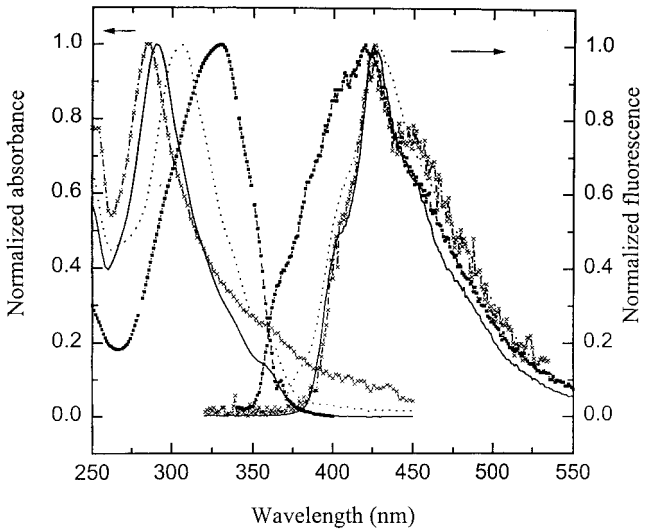

Figure 4. Absorption and fluorescence spectra of TS_8A, TS_8EPC, and TS_4EPC in different media: — TS_8EPC in water, ••• TS_4EPC in water, —×— TS_8A monolayer, - - - TS_8A in γ-CD.

On the basis of the general similarities between the TS amphiphiles and the well-studied *trans*-stilbene derivatives, it appears reasonable to assign the shifted absorption and fluorescence spectra obtained in the pure phospholipid aqueous dispersions and Langmuir−Blodgett films of TS_8A, TS_8EPC, and TS_4EPC to "H" aggregates in which the TS chromophores are packed with their long-axis polarized transitions parallel. The slightly broadened absorption spectra obtained for the TS phospholipid dispersions in the presence of excess DMPC can also be assigned to a dimer by analogy to the results obtained for the stilbene derivatives[2] and from the similar spectrum obtained for TS_8A in the presence of γ-cyclodextrin. This suggests that the aggregates obtained in the pure dispersions must be larger than dimers. As shown in Figure 4, the absorption spectrum for TS_4EPC in water is broader and significantly less blue-shifted than that for TS_8EPC in water while the monolayer of TS_8A shows the most pronounced blue-shift. It has previously been shown that the extent of the blue-shift in the absorption spectra can be roughly correlated with the aggregate size.[2] The larger blue-shifts observed for the monolayers and LB films of TS_8EPC and TS_8A compared to

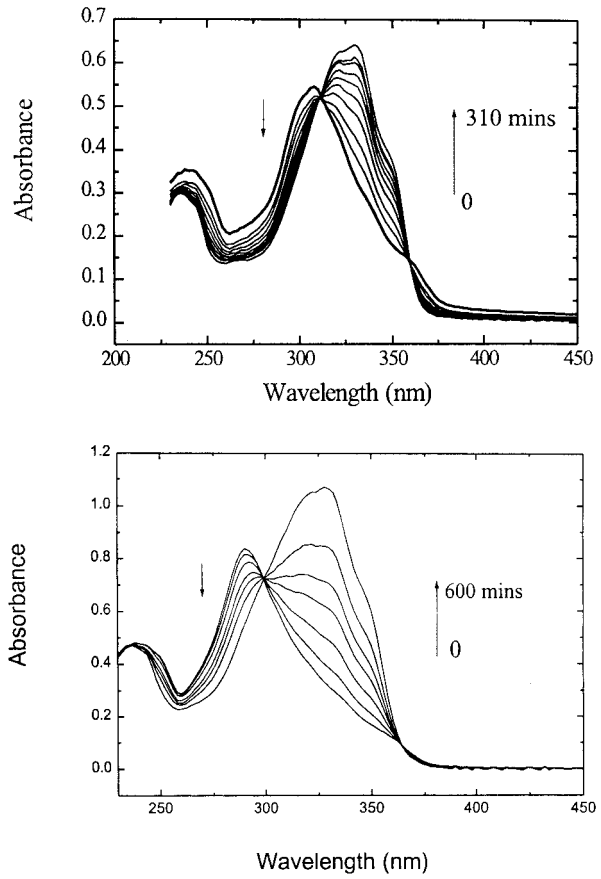

Figure 5. Time evolution of absorption spectra of TS_4EPC (upper) and TS_8EPC (lower) assemblies in water when treated with DMPC vesicles.

TS_4EPC aqueous dispersions suggest relatively extended aggregates in the former and smaller aggregates in the latter.

Studies of Details of Aggregation of Styrylthiophenes in Aqueous Dispersions. As has been found with azobenzene- and stilbene-derivatized phospholipids, mixing of pure aqueous dispersions of the substituted phospholipid with aqueous dispersions of pure saturated phospholipids, in large excess, leads to disaggregation of the "H" aggregates to dimer (or monomer for phospholipids containing only a single chromophore).[2,3] The presence of isosbestic points during the conversion has been taken as evidence that clean evolution from an aggregate of definite size to the dimer occurs during the process. As shown in Figure 5, similar spectral changes occur for both TS_8EPC and TS_4EPC with DMPC. For the previously studied modified phospholipids,[2,3] it was found that this sort of "membrane exchange" process occurs only above the phase transition temperature, T_c, for both of the phospholipids undergoing the mixing. In the present studies it was found that the exchange could be observed only at or above 60° C for TS_8EPC and above 30° C for TS_4EPC, implying that the two phospholipids exhibit the chain-melting transition at these temperatures. The disaggregation process follows first-order kinetics (independent of [DMPC]), suggesting extrusion of an individual phospholipid from the aggregate is the rate-limiting step. Table 2 gives equilibrium and rate constants for the disaggregation process. From the equilibrium constants, a modified Benesi−Hildebrand relationship[2,23] (Figure 6) was used to determine the aggregation numbers; in terms of phospholipid molecules, these were found to be 2.02 and 5.96 for TS_4EPC and TS_8EPC, respectively. In terms of TS chromophores these correspond to 4 and 12, respectively, for the two phospholipids. A plot of ln K vs $1/T$ for TS_4EPC over the temperature range 35−55° C shows good linearity and enables an estimate of $\Delta H = 19.5$ kcal/mol and $\Delta S = 55$ cal/mol K for the disaggregation. The results for TS_4-EPC may be compared with the corresponding *trans*-stilbene phospholipid S_4EPC,[2] which also forms relatively small aggregates. Both the enthalpy (ca. 5 kcal/mol/chromphore) and entropy (ca. 15 cal/mol K/molecule) as well as the rate constants for disaggregation (2×10^{-2} min^{-1} for S_4EPC at 30 °C and 2.1×10^{-2} min^{-1} for TS_4EPC at 32 °C) are similar even though the aggregation numbers are different.

TABLE 2: Equilibrium and Rate Constants for Deaggregation Process

	T (°C)	k ($\times 10^3$ min^{-1})	K ($\times 10^2$)
TS_8EPC	50	1.0	
	55		1.2×10^{-5}
	60	7.0	
TS_4EPC	32	2.1	
	35		1.78
	40		2.26
	45		4.34
	50		7.62
	55		11.8

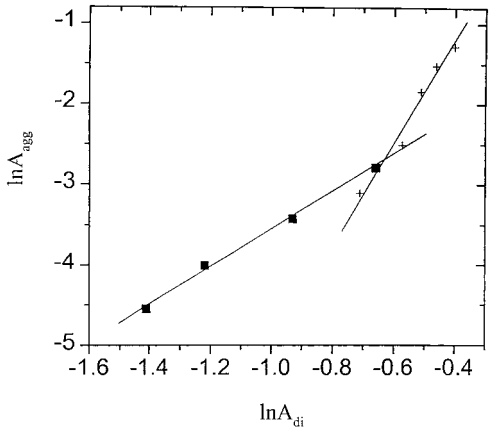

Figure 6. Benesi−Hildebrand plot of ln A_{agg} as a function of ln A_{di} for TPLs in DMPC vesicles: ■ TS_4EPC at 35 °C, + TS_8EPC at 55 °C.

As was also the case with the pure dispersions of azobenzene- and stilbene-phosphatidyl choline derivatives,[2,3] the styrylthiophene phospholipid pure aqueous dispersions give evidence of forming structures that may be much larger than those for simple saturated phospholipids and perhaps of quite different shapes. Thus while dipalmitoyl phosphatidyl choline has an approximate size (diameter, for small unilamellar vesicles) of 9.3 nm,[24a] the stilbene phospholipids have sizes estimated by light scattering or membrane filtration in the range 200−500 nm. Similarly, membrane extrusion experiments indicate sizes of approximately 150 and 100 nm for dispersions of TS_4EPC and TS_8EPC, respectively. As indicated above, phase transition temperatures may be roughly indicated by the temperatures at which mixing occurs readily with DMPC ($T_c = 20.9$ °C);[24b] for TS_8EPC there is also a sharp discontinuity in a plot of fluorescence efficiency vs T at 60°, which supports a chain-melting occurrence in this range.

Although the TS phospholipids are chiral (prepared from α-glyceryl phosphatidyl choline), there is no induced circular dichroism (ICD) in the region of the TS chromophore absorptions when the phospholipids are dissolved in organic solvents such as chloroform. However, for the aqueous dispersions of both TS_4EPC and TS_8EPC, there is a strong biphasic (excitonic) ICD in the regions of the aggregate absorption with a crossover

point coinciding with the absorption maximum. The apparent molar ellipticity of the TS_4EPC dispersion is more than one-third higher than that of the TS_8EPC dispersion, which may reflect either a larger asymmetry of the smaller aggregate for the former or a shorter distance between the chromophore and the chiral headgroup or a combination of both factors.

Photophysics and Photochemistry of Styrylthiophene Phospholipids in Solution and Aqueous Dispersions. As shown in Table 1, the fluorescence quantum yields are relatively low (a few percent) in organic solutions but increase to the range 10−30% in aqueous dispersions. The fluorescence decays in chloroform are found to be monoexponential with very short lifetimes (23 ps for TS_4EPC and 29 ps for TS_8EPC, close to the limit of instrument resolution). For the cyclodextrin complexes of TS_8A, it was found that the monomer in α-cyclodextrin has a fluorescence efficiency of 0.24, while for *β*-cyclodextrin, the fluorescence efficiency is 0.03, similar to the chloroform solution, while the "dimer" in *γ*-cyclodextrin shows a fluorescence quantum yield of 0.2. As has been found for other aqueous dispersions of aggregated fluorescent chromophores,[2,5] the fluorescence decay of dispersions of the styrylthiophene phospholipids are complicated; in each case the fluorescence can be fit into three lifetime distributions. The measured distributions are similar; in each case there is an extremely short lifetime distribution (20−100 ps), which is of negligible percentage and could be attributed to either monomer or an artifact. A second distribution, 0.34 ns and 25% for TS_4-EPC and 0.2 ns and 35% for TS_8EPC, and third distribution, 2.7 ns for TS_4EPC (75%) and 4.8 ns for T_8EPC (65%), comprise most of the decay and can be tentatively assigned to aggregate and excimer (see below), respectively, in accord with the similar assignments for the stilbene phospholipids.[2]

The styrylthiophenes are photoactive in both organic solutions and aqueous dispersions. Relatively efficient photoisomerization from *trans* to *cis* occurs upon irradiation of chloroform solutions at 365 nm, which was confirmed by the appearance of signals attributed to the new *cis* protons in ^{1}H NMR. This is consistent with the reported results for irradiation of simple styrylthiophenes in benzene.[18] The *cis* isomers are thermally stable at room temperature. Both of the styrylthiophene phospholipids undergo photobleaching upon irradiation of the aggregate band in aqueous dispersions. As shown in Figure 7 for TS_4EPC aqueous dispersions, the photobleaching coincides with a disappearance of the ICD bands; the net efficiency of the photobleaching is about one-sixth that of the photoisomerization in chloroform. The product from irradiation of aqueous dispersions of TS_4EPC was isolated and analyzed. The process involved hydrolyzing the crude product to cleave the phosphatidylcholine residue and reesterification of the product acid. The major photoproduct was studied by ^{1}H NMR and FAB mass spectroscopy and found to be a photodimer, which can be assigned as either **1** or **3** of the four possible dimers resulting from cyclodimerization of two *trans*-styrylthiophenes. (Chart 3) This structural assignment was based upon the symmetrical cyclobutane AA′BB′ multiplets centered at *δ* 4.55 for the ^{1}H NMR of the major product and literature reports for structurally related photodimer sets.[25] The presence of only one major photodimer from the aqueous dispersions clearly attests to a well-ordered packing structure in the aggregates.[16] The excitation and fluorescence spectra of the TS phospholipid aqeuous dispersions show interesting changes as the irradiation proceeds. They remain effectively unchanged through the major portion of the irradiation (except for a decrease in intensity; the products do not fluoresce). However, at late stages (∼90% reaction) the fluorescence spectra become broader and are similar to that of the excimer observed for TS_8A in *γ*-cyclodextrin. The excitation spectra also shift to the red and could be attributed to either the monomer or dimer (Figure 8). Another interesting change that accompanies photodimerization of the aqueous dispersions of pure TS_4EPC or TS_8EPC is a reduction in size of the assemblies. Thus while no TS_8EPC would pass through a

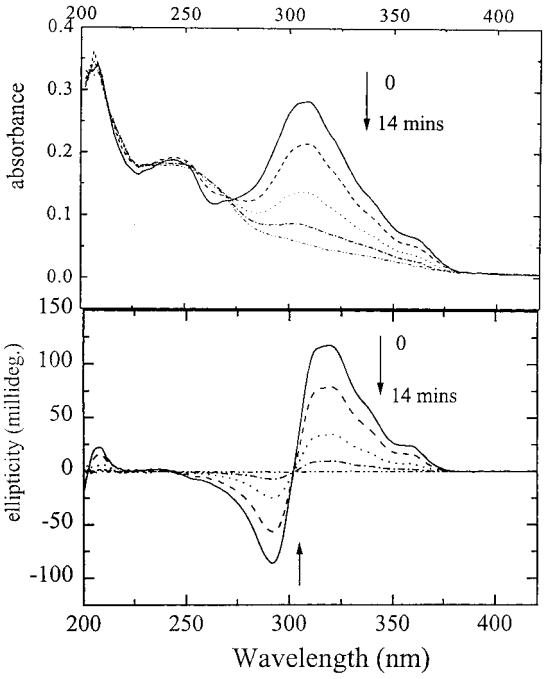

Figure 7. (upper) Absorption and (lower) ICD spectra of TS_4EPC aqueous dispersion upon irradiation at 365 nm.

CHART 3

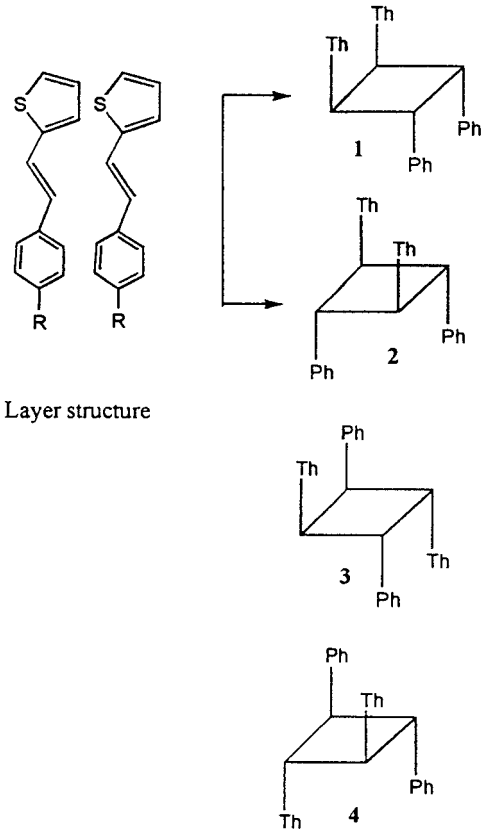

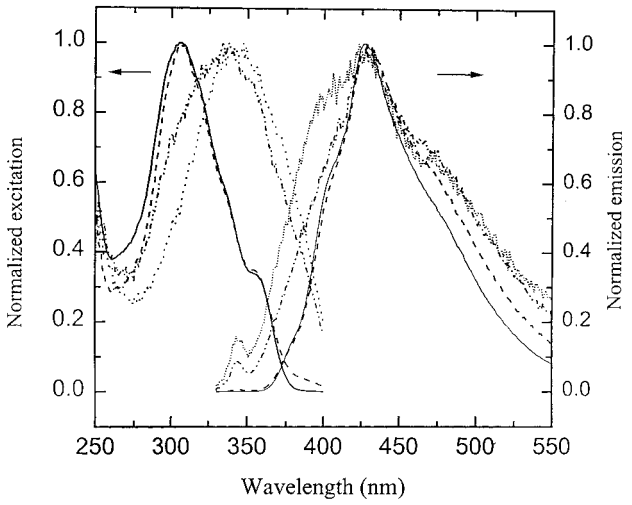

Figure 8. Emission and excitation spectra of TS_4EPC aqueous dispersion upon photobleaching: — 0 min, - - - 16 min, —···— 26 min, ··· 36 min.

polycarbonate membrane with 100-nm pores, the photoproduct from the dispersion could pass completely through the same membrane.

Reagent Entrapment and Photorelease from Vesicles Containing Styrylthiophene Phospholipids. While the pure dispersions of TS_4EPC and TS_8EPC are not able to entrap water soluble reagents such as carboxyfluorescein (CF), presumably because they do not exist as simple bilayer vesicle structures, mixtures of DPPC with small amounts of the styrylthiophene phospholipid TS_8EPC do form evidently closed structures that can entrap carboxyfluorescein for prolonged periods (more than one week) in the dark. Particularly interesting results were observed for incorporation of TS_8A and TS_8EPC in DPPC to form vesicles with carboxyfluorescein entrapped on the inside at a concentration high enough to ensure efficient self-quenching.[26] Only a small percentage (<3 mol %, but primarily aggregate) of TS_8EPC in the DPPC vesicle is needed to produce almost total release of the entrapped CF upon photolysis at 365 nm. In contrast, incorporation of TS_8A to a level of >10 mol % (mostly monomer) results in only a small amount of release (<10%) upon photolysis under the same conditions. The pattern of release for the TS_8EPC—DPPC dispersions is similar to that observed for photorelease of entrapped CF from azobenzene phospholipid aggregate—DPPC dispersions and suggests a "catastrophic" mechanism for destruction of the vesicle structure.[3]

Monte Carlo Simulations of the Structure of Styrylthiophene Fatty Acid Clusters: Relevance to the Structure of the Aggregate in LB Films and Phospholipid Dispersions. Additional information concerning possible aggregate structures in the assemblies of the styrylthiophene amphiphiles can be obtained by examining possible packing geometries using Monte Carlo cooling simulations. The detailed procedures for the structural predictions and the technique have been reported elsewhere.[4b,27] The simulated packing of TS_4A and TS_8A into monolayers was accomplished by applying Kitaigorodskii's Aufbau principle (KAP)[28] to a Monte Carlo simulation using the MM2 force field. The predicted spectral shifts resulting from exciton interaction for the simulated structures were calculated using the extended dipole—extended dipole method developed by Kuhn and co-workers.[11] For this computation a transition moment of 7.07 D was estimated from the oscillator strength of the styrylthiophene monomer in chloroform at 332 nm with an approximate classical dipole length of 8.9 Å, estimated from the carbon—carbon end-to-end distance for *trans*-styrylthiophene. The dielectric constant was assumed to be 2.5. The exciton splitting was computed by summing the interaction energy of the dipoles over the monolayer lattice. Convergence was achieved by the time 14 × 14 unit cells were included in the computation. Table 3 summarizes data for the lowest energy translation and glide structures predicted for TS_8A, while Table 4 gives data for the lowest energy structures predicted for TS_4A. The predictions are somewhat different for the two fatty acids. Thus for TS_8A the lowest energy structures are all translation layers; of those the ones of rank 1 and 3 show good agreement in terms of the predicted absorption spectra for the aggregate and the measured area/molecule. The glide layer structure of rank 10 also shows reasonable agreement with the measured properties. Figure 9 compares overhead views of the simulated structures of rank 1 (translation) and 10 (glide). For the simulated structures of TS_4A the lowest energy structures are a mix of glide and translation layers. Although TS_4A is too water soluble to study as a film at the air—water interface, a reasonable assumption is that the area/molecule in the compressed monolayer would be approximately the same as that for TS_8A.

TABLE 3: Simulated Two-Dimensional Layer Structures for TS_8A

rank	type[a]	a[b]	c[b]	β[b]	area[c]	λ_1[d]	λ_2[d]	ratio[d]	energy
0	t	5.27	4.12	83.70	21.58	298			−31.02
1	t	5.25	4.42	96.95	23.03	290			−30.15
2	t	5.61	4.34	94.79	24.26	306			−30.06
3	t	5.27	4.44	98.47	23.14	290			−29.03
4	t	4.28	6.06	71.03	24.53	304			−28.20
5	t	6.75	4.12	78.29	27.23	311			−27.41
6	g	6.55	8.23	90.00	26.95	308	338	0.04	−24.52
7	g	6.46	8.23	90.00	26.38	305	338	0.02	−24.52
8	g	7.75	9.55	90.00	37.01	342	345	0.00	−22.82
9	g	6.83	10.79	90.00	36.85	340	338	22.6	−22.63
10	g	6.15	7.39	90.00	22.72	295	339	0.02	−22.20
exptl					23.0	290			

[a] t = translation layer structure, g = glide layer structure. [b] a, c, β are predicted unit cell dimensions in Å and angle in deg between a and c, respectively. The value of 90° for glide layers is assumed (not predicted) because the glide layer space group requires it. See ref 28 for details of the unit cell symmetries for glide and translation layers and ref 15 for pictorials. [c] Surface area in Å^2 per molecule. [d] λ_1 and λ_2 are computed spectral peaks from exciton coupling and the ratio of the long-wavelength predicted intensity to the short-wavelength predicted intensity using the extended dipole approximation of Kuhn et al. (ref 11).

TABLE 4: Simulated Two-Dimensional Layer Structures for TS_4A

rank	type[a]	a[b]	c[b]	β[b]	area[c]	λ_1[d]	λ_2[d]	ratio[d]	energy
0	t	5.59	4.31	94.86	24.01	300			−29.39
1	g	6.89	6.49	90.00	22.36	297	338	0.18	−28.31
2	t	5.90	4.25	95.09	24.98	303			−27.82
3	t	5.52	4.06	92.11	22.40	294			−27.34
4	t	5.56	4.34	100.23	23.75	293			−27.29
5	g	6.70	7.12	90.00	23.85	298	338	0.10	−27.21
6	t	6.14	4.31	85.08	26.37	307			−26.72
7	g	6.81	7.18	90.00	24.45	296	339	0.01	−26.64
8	g	6.41	8.07	90.00	25.86	304	338	0.06	−26.59
9	t	6.12	4.07	79.66	24.50	305			−26.30
10	t	4.96	4.66	86.15	23.06	300			−26.29
exptl					23	290			

[a] t = translation layer structure, g = glide layer structure. [b] a, c, β are unit cell in Å and deg. [c] Surface area in Å^2 per molecule. [d] λ_1 and λ_2 are computed spectral peaks from exciton coupling and the ratio of the long-wavelength predicted intensity to the short-wavelength predicted intensity using the extended dipole approximation of Kuhn et al. (ref 11).

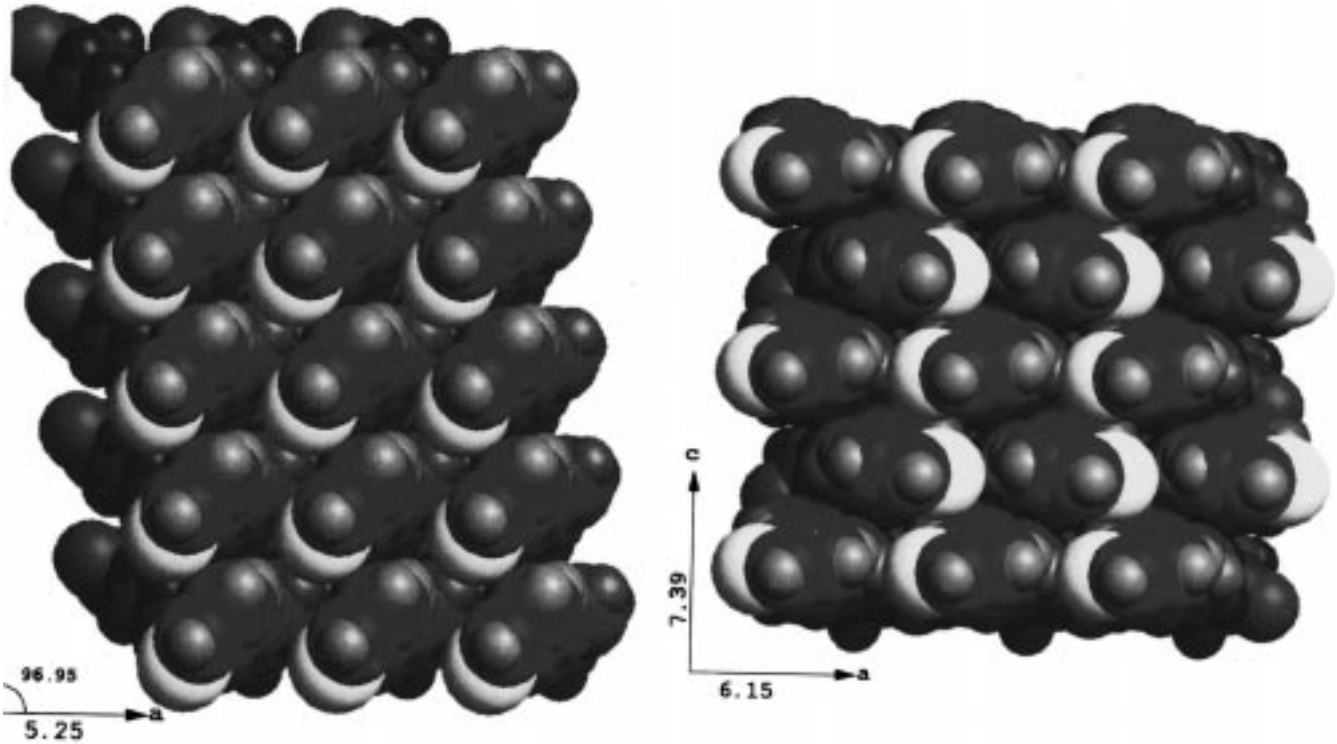

Figure 9. (a, left) Rank 1 translation layer of TS_8A. View is looking down on the layer from the thiophene side showing the packing of the thiphene groups (sulfur in yellow, carbon in green). Cell dimensions of the layer in angstroms, angles in degrees. (b, right) TS_8A glide layer rank 10. View is also from the thiphene side. The glide direction is along the *c*-axis.

Several low-energy structures (all within 3 kcal/mol of each other in energy) are either glide or translation; however, in terms of agreement between experimental and predicted parameters for TS_8A, there is little basis to favor any specific structure.

Discussion

From the experimental results presented above, it would seem reasonable to infer that the styrylthiophene phospholipids and fatty acids form aggregates of similar strength and structure to those observed previously for *trans*-stilbene and azobenzene amphiphiles.[2,3] In particular, the aggregation numbers observed (4 and 12), enthalpy and entropy of dissociation, absorption spectral shifts, and structured fluorescence are all consistent with a "supramolecular" unit aggregate. A reasonable structure might be a "pinwheel" tetramer[2−4] characterized by edge−face association of the chromophores (Figure 1) similar to those deduced for the structurally similar stilbene and azobenzenes and for the somewhat different squaraines. The packing together of "pinwheel" unit aggregates readily generates an extended glide or herringbone lattice, as has been pointed out previously. We have found that crystals of several amphiphilic *trans*-stilbene derivatives have structure of this type, which closely resemble Langmuir−Blodgett multilayers.[15] However, the observation of clean photochemical reaction in the pure aqueous suspensions of the styrylthiophene phospholipids to produce what is most reasonably assigned as the syn head-to-head photodimer appears much more consistent with a topologically controlled process, which can be envisioned to occur most readily from a translation layer arrangement of the chromophores in which there is a parallel or face−face arrangement of the chromophores,[29] such as in the simulated translation layer structure shown in Figure 9a. In this regard the photodimerization appears closely related to that observed for crystals of molecules such as the cinnamic acid derivatives[30] or monolayer films and phospholipid suspensions of amphiphilic styrene derivatives.[16]

The molecular simulations suggest that glide and translation layer structures may be relatively close in energy for the corresponding fatty acid monolayers and that the spectral shifts observed and other properties might be accommodated by either a translation or glide structure. Since these simulations are for gas-phase structures and do not take into account possible interactions between water and the headgroups, it is quite possible that solvent interactions may alter the relative energies; thus, it is reasonable to consider any of the structures listed in Tables 3 and 4 as potentially accessible or even global minimum energy configurations. In fact, given the anticipated somewhat more dynamic nature of the aqueous phospholipid bilayer suspensions in water compared to crystals or condensed LB films or supported multilayers, it seems possible that for the former oscillation or equilibration between differing assembly minima may take place. Thus it is reasonable that the "true" structure of the aqueous phospholipid dispersions might consist of equilibrating glide and translation structures or oscillating translation layer structures or both or a more complex array. The fact that the absorption spectra show relatively little variation with temperature might be taken as evidence either that there are not dramatic differences in chromophore−chromophore interactions in differing contributing ensembles or that the composition does not vary substantially over the temperature range examined. The observation that photodimerization occurs in the aqueous phospholipid dispersions may also be attributed to dynamic possibilities not available for crystals or even LB multilayers. Thus for TS_8A and TS_4A only one of the simulated low-energy translation layer structures having reasonable agreement with measured parameters (structure of rank 9 for TS_4A in Table 4) has double bonds in adjacent molecules within the "magic distance" limit of 4.2 Å.[17,30] The necessity for motion within the ensemble to bring adjacent molecules close enough to dimerize may be one reason for the

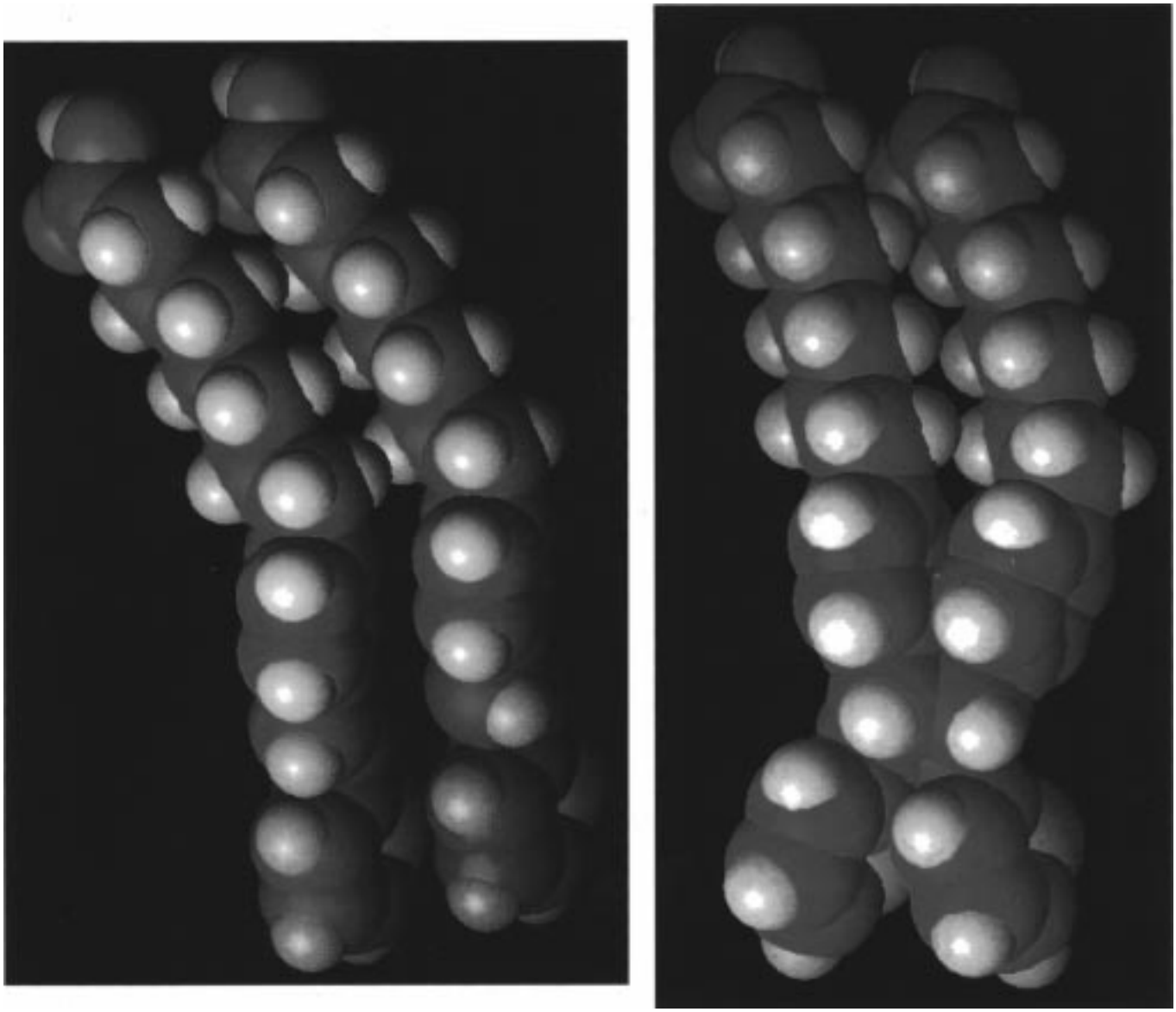

Figure 10. (a, left) Simulated structure of TS_8A from rank 1 translation layer (Table 3); (b, right) simulated structure of resultant syn-head−head photodimer.

relatively low quantum yield for dimerization compared to the solution-phase isomerization yield.

One of the more interesting findings in this study is that photolysis of mixed bilayer vesicles (TS_8EPC:DPPC) under conditions where the photolysis should convert aggregates styrylthiophene monomer to photodimer results in release of reagents entrapped within the vesicles. If photodimerization were a simple topologically controlled process that resulted in little change of shape and size of the reacting pair, it would be anticipated that little disruption of the vesicle macrostructure would result. Clearly this is not the case, since the photoinduced release that occurs is quite comparable in both extent and speed to that produced by irradiation of *trans*-azobenzene aggregates.[3] Further evidence that photodimerization of the aggregated styrylthiophene results in major structural disruption is found by examining the effective size of the phospholipid dispersions, prior and subsequent to photodimerization. The relatively large structures retained upon filtration through a 100-nm membrane are clearly disrupted as the photodimerization occurs. The change in the residual absorption and emission spectra as photodimerization proceeds also supports the idea that major structural rearrangments occur as monomer is converted to photodimer. Figure 10 compares simulated structures of a pair of TS_8A molecules in the rank 1 translation layer before and after formation of the syn head-to-head photodimer. Although the area of the photodimer is slightly smaller than that of the pair of monomers, the shape is quite different as is the "π"-surface exposed to adjacent molecules. Both of these changes that occur upon photodimerization might be expected to play important roles in destabilizing the aggregate structure. The observation that "excimer" fluorescence becomes prominent as high conversion to photodimer occurs in pure dispersions suggests the possibility that the "defect" introduced by conversion of two monomers to a photodimer may facilitate the collapse of "aggregate" excited states to "excimer" and actually accelerate photodimerization at moderate-to-high conversion. Since the assessment of quantum yields for reaction at moderate to high conversion cannot be carried out with any precision, it is very hard to test this possibility. A perhaps more interesting possibility is that the formation of photodimers in a mosaic of aggregate results in weakened noncovalent interactions between the π-systems and at some stage to a complete collapse of the aggregate "mosaic". This would be consistent with the photodimerization producing a similar "catastrophic" destruction

of the vesicle structure somewhat similar to that when aggregated azobenzene is photoisomerized but not when the photoisomerization involves an isolated azobenzene monomer.

One of the interesting questions that is raised by the finding of relatively strong attractive noncovalent interactions between the chromophores in the modified amphiphiles examined in this and related studies is whether there are specific π-interactions that govern the strength and structure of the assemblies or if it is much more shape and topology that play decisive roles. We are currently seeking to address these questions so as to be able to develop and control more closely the coupling of monomer structure with ensemble properties.

Acknowledgment. We thank the U.S. National Science Foundation (Grant Number CHE-9521048) for generous support of this research.

References and Notes

(1) Whitten, D. G. *Acc. Chem. Res*. **1993**, *26*, 502.

(2) (a) Song, X.; Geiger, C.; Furman, I.; Whitten, D. G. *J. Am. Chem. Soc*. **1994**, *116*, 4103. (b) Song, X.; Geiger, C.; Leinhos, U.; Perlstein, J.; Whitten, D. G. *J. Am. Chem. Soc*. **1994**, *116*, 10340.

(3) (a) Song, X.; Perlstein, J.; Whitten, D. G. *J. Am. Chem. Soc*. **1995**, *117*, 7816. (b) Song, X.; Perlstein, J.; Whitten, D. G. *J. Am. Chem. Soc*. **1997**, *119*, 9144.

(4) (a) Chen, H.; Farahat, M.; Law, K. Y.; Perlstein, J.; Whitten, D. G. *J. Am. Chem. Soc*. **1996**, *118*, 2586. (b) Chen, H.; Law, K. Y.; Perlstein, J.; Whitten, D. G. *J. Am. Chem. Soc*. **1995**, *117*, 7257.

(5) Farahat, C. W.; Penner, T. P.; Ulman, A.; Whitten, D. G. *J. Phys. Chem*. **1996**, *100*, 12616.

(6) (a) Furman, I.; Geiger, H, C.; Whitten, D. G.; Penner, T. L.; Ulman, A. *Langmuir* **1994**, *10*, 837. (b) Morgan, C. G.; Thomas, W. E.; Moras, T. S.; Yianni, Y. P. *Biochim. Biophys. Acta* **1982**, *692*, 196.

(7) Chen, H.; Liang, K. L. Song, X.; Samha, H.; Law, K. Y.; Perlstein, J.; Whitten, D. G. In *Micelles, Microemulsions, and Monolayers*: *Science and Technology*; Shah, D., Ed.; Marcel Dekker, Inc: New York, in press.

(8) Kunitake, T. *Angew. Chem., Int. Ed. Engl*. **1992**, 709−726.

(9) (a) Schweitzer, B. A.; Kool, E. T. *J. Am. Chem. Soc*. **1995**, *117*, 1863. (b) Winnik, F. M. *Chem. Rev*. **1993**, *93*, 587. (c) Hunter, C. A.; Saunders: J. K. M. *J. Am. Chem. Soc*. **1990**, *112*, 5525. (d) Jorgenson, W. L.; Severance, D. L. *J. Am. Chem. Soc*. **1990**, *112*, 4768.

(10) (a) Arunan, E.; Gutowsky, H. S. *J. Chem. Phys*. **1993**, *98*, 4294. (b) Hall, D.; Williams, D. F. *Acta Crystallogr*. **1975**, *A31*, 56.

(11) (a) Czikkely, V.; Fîrsterling, H.; Kuhn, H. *Chem. Phys. Lett*. **1970,** *6*, 11. (b) Czikklely, V.; Fîrsterling, H. D.; Kuhn, H. *Chem. Phys. Lett.* **1970,** *6*, 207.

(12) Geiger, H. C.; Saeva, F. D.; Whitten, D. G. Manuscript in preparation.

(13) (a) Murata, K.; Aoki, M.; Suzuki, T.; Harada, T.; Kawabata, H.; Komori, T.; Ohseto, F.; Ueda, K.; Shinkai, S. *J. Am. Chem. Soc.* **1994,** *116*, 6664. (b) Murata, K.; Aoki, M.; Nishi, R.; Ikeda, A.; Shinkai, S. *J. Chem. Soc., Chem. Commun.* **1991**, 1715.

(14) Stanescu, M. Unpublished results.

(15) Vaday, S.; Geiger, H. C.; Cleary, B.; Perlstein, J.; Whitten, D. G. *J. Phys. Chem*. **1997**, *101*, 321.

(16) Zhao, X.; Perlstein, J.; Whitten, D. G. *J. Am. Chem. Soc*. **1994**, *116*, 10463.

(17) Schmidt, G. M. J. *Pure Appl. Chem.* **1971,** *27*, 647. Kaupp, G. *CRC Handbook of Organic Photochemistry and Photobiology*; Horspool, W. M., Song, P.-S., Eds.; CRC Press: Boca Raton, FL, 1995; p 50.

(18) Kellogg, R. M.; Groen, M. B.; Wynberg, H. *J. Org. Chem*. **1967**, *32*, 3093.

(19) (a) Robertson, J. M.; Woodward, I. *Proc. R. Soc. London, Ser. A* **1937**, *162*, 568. (b) Schmidt, G. M. *Photoreactivity of the Photoexcited Organic Molecules*; Interscience: New York, 1967; p 227.

(20) Kuhn, H.; Môbius, D.; Böcher, H. In *Physical Methods of Chemistry*; Weissberger, A., Rossiter, B. W., Eds.; Wiley: New York, 1972; Vol. 1, p 577.

(21) (a) Hope, M. J.; Bally, M. B.; Webb, G.; Cullis, P. R. *Biophys. Acta* **1985**, *55*, 812. (b) Saunders: L.; Perrin, J.; Gammock, D. B. *J. Pharm. Pharmacol*. **1962**, *14*, 567.

(22) Morgan, C. G.; Thomas, W. E.; Moras, T. S.; Yianni, Y. P. *Biochim. Biophys. Acta* **1982**, *692*, 196.

(23) Benesi, H. A.; Hildebrand, J. H. *J. Am. Chem. Soc*. **1949,** *71*, 2703.

(24) (a) Watts, A.; Marsh, D.; Knowles, P. F. *Biochemistry* **1978**, *17*, 1792−1801. (b) Lentz, B. R.; Barenholz, Y.; Thompson, T. E.; *Biochemistry* **1976**, *15*, 4521.

(25) Green, B. S.; Heller, L.; *J. Org. Chem*. **1974**, *39*, 196−201.

(26) Weinstein, T. N.; Yoshikamii, S.; Henkart, P.; Blumenthal, R.; Hagins, W. A. *Science* **1977**, *195*, 489.

(27) (a) Perlstein, J. *J. Am. Chem. Soc*. **1994,** *116*, 455. (b) Perlstein, J. *J. Am. Chem. Soc*. **1994,** *116*, 11420.

(28) Kitaigorodskii, A. I. *Organic Chemical Crystallography*; Consultants Bureau: New York, 1961; pp 65−112.

(29) Interestingly, some of the low-lying glide layer structures have a face−face arrangement of styrylthiophene chromophores such that the double bonds might be close enough to permit photodimerization to occur; however, in this case topological control would be expected to result in formation of the anti head-to-head dimer, which is clearly not formed as a major product.

(30) Ramamurthy, V.; Venkatesan, K. *Chem. Rev.* **1987**, *87*, 433. Cohen, M. D. *Mol. Cryst. Liq. Cryst.* **1979**, *50*, 1.